

# Epidermal Growth Factor Receptor-targeted $^{131}\text{I}$ -therapy of Liver Cancer Following Systemic Delivery of the Sodium Iodide Symporter Gene

Kathrin Klutz<sup>1</sup>, David Schaffert<sup>2</sup>, Michael J Willhauck<sup>1</sup>, Geoffrey K Grünwald<sup>1</sup>, Rudolf Haase<sup>2</sup>, Nathalie Wunderlich<sup>1</sup>, Christian Zach<sup>3</sup>, Franz J Gildehaus<sup>3</sup>, Reingard Senekowitsch-Schmidtke<sup>4</sup>, Burkhard Göke<sup>1</sup>, Ernst Wagner<sup>2</sup>, Manfred Ogris<sup>2</sup> and Christine Spitzweg<sup>1</sup>

<sup>1</sup>Department of Internal Medicine II, Ludwig-Maximilians-University, Munich, Germany; <sup>2</sup>Department of Pharmacy, Center of Drug Research, Pharmaceutical Biotechnology, Ludwig-Maximilians-University, Munich, Germany; <sup>3</sup>Department of Nuclear Medicine, Ludwig-Maximilians-University, Munich, Germany; <sup>4</sup>Department of Nuclear Medicine, Technical University, Munich, Germany

We recently demonstrated tumor-selective iodide uptake and therapeutic efficacy of radioiodine in neuroblastoma tumors after systemic nonviral polyplex-mediated sodium iodide symporter (NIS) gene delivery. In the present study, we used novel polyplexes based on linear polyethylenimine (LPEI), polyethylene glycol (PEG), and the synthetic peptide GE11 as an epidermal growth factor receptor (EGFR)-specific ligand to target a NIS-expressing plasmid to hepatocellular carcinoma (HCC) (HuH7). Incubation of HuH7 cells with LPEI-PEG-GE11/NIS polyplexes resulted in a 22-fold increase in iodide uptake, which was confirmed in other cancer cell lines correlating well with EGFR expression levels. Using  $^{123}\text{I}$ -scintigraphy and *ex vivo*  $\gamma$ -counting, HuH7 xenografts accumulated 6.5–9% injected dose per gram (ID/g)  $^{123}\text{I}$ , resulting in a tumor-absorbed dose of 47 mGy/Megabecquerel (mGy/MBq)  $^{131}\text{I}$  iodide ( $^{131}\text{I}$ ) after intravenous (i.v.) application of LPEI-PEG-GE11/NIS. No iodide uptake was observed in other tissues. After pretreatment with the EGFR-specific antibody cetuximab, tumoral iodide uptake was markedly reduced confirming the specificity of EGFR-targeted polyplexes. After three or four cycles of polyplex/ $^{131}\text{I}$  application, a significant delay in tumor growth was observed associated with prolonged survival. These results demonstrate that systemic NIS gene transfer using polyplexes coupled with an EGFR-targeting ligand is capable of inducing tumor-specific iodide uptake, which represents a promising innovative strategy for systemic NIS gene therapy in metastatic cancers.

Received 8 September 2010; accepted 9 December 2010; published online 18 January 2011. doi:10.1038/mt.2010.296

## INTRODUCTION

The growing understanding of the biology of the sodium iodide symporter (NIS) since its cloning in 1996 has paved the way for

the development of a novel cytoreductive gene therapy strategy using *NIS* as powerful therapy and reporter gene.<sup>1</sup> *NIS*, an intrinsic transmembrane glycoprotein with 13 putative transmembrane domains, is responsible for the ability of the thyroid gland to concentrate iodide, the first and rate-limiting step in the process of thyroid hormonogenesis.<sup>2</sup> Moreover, due to its expression in follicular cell-derived thyroid cancer cells, *NIS* provides the molecular basis for the diagnostic and therapeutic application of radioiodine, which has been successfully used for >70 years in the treatment of thyroid cancer patients representing the most effective form of systemic anticancer radiotherapy available to the clinician today.

After extensive preclinical evaluation in several tumor models by various groups including our own, *NIS* has been characterized as a promising target gene for the treatment of nonthyroid cancers following selective *NIS* gene transfer into tumor cells which allows therapeutic application of radioiodine and alternative radionuclides, such as  $^{188}\text{Re}$  and  $^{211}\text{At}$  ( $^{211}\text{At}$ ).<sup>1–4</sup> In our initial studies in the prostate cancer model, we used the prostate-specific antigen promoter to achieve prostate-specific iodide accumulation, which resulted in a significant therapeutic effect after application of  $^{131}\text{I}$  iodide ( $^{131}\text{I}$ ) and alternative radionuclides such as  $^{188}\text{Re}$  and  $^{211}\text{At}$  even in the absence of iodide organification.<sup>3–6</sup> Furthermore, cloning of *NIS* has also provided us with one of the most promising reporter genes available today, that allows direct, noninvasive imaging of functional *NIS* expression by  $^{123}\text{I}$ -scintigraphy and  $^{124}\text{I}$ -positron emission tomography ( $^{124}\text{I}$ -PET)-imaging, as well as exact dosimetric calculations before proceeding to therapeutic application of  $^{131}\text{I}$ . Therefore, in its role as reporter gene *NIS* provides a direct way to monitor the *in vivo* distribution of viral and nonviral vectors, as well as biodistribution, level, and duration of transgene expression—all critical elements in the design of clinical gene therapy trials.<sup>2,3,5,7–17</sup>

As logical consequence of our pioneer studies in the *NIS* gene therapy field, the next crucial step toward clinical application of the promising *NIS* gene therapy concept, has to be the evaluation of

**Correspondence:** Christine Spitzweg, Medizinische Klinik II—Campus Grosshadern, Klinikum der Universität München, Marchioninistrasse 15, 81377 Munich, Germany. E-mail: [Christine.Spitzweg@med.uni-muenchen.de](mailto:Christine.Spitzweg@med.uni-muenchen.de) or Manfred Ogris, Department of Pharmacy, Center of Drug Research, Pharmaceutical Biotechnology, Butenandtstrasse 5-13, 81377 Munich, Germany. E-mail: [Manfred.Ogris@cup.uni-muenchen.de](mailto:Manfred.Ogris@cup.uni-muenchen.de)

gene transfer methods that have the potential to achieve sufficient tumor-selective transgene expression levels not only after local or regional but also after systemic application to be able to reach tumor metastases.

Delivering genes to target organs with synthetic vectors is a vital alternative to virus-based methods. For systemic delivery, polycationic molecules are used to condense DNA into submicrometer particles termed polyplexes, which are efficiently internalized into cells, while DNA is protected from nucleases. Several polycations, like polyethylenimine (PEI), bear an intrinsic endosomolytic mechanism, which allows the transition of the polyplex from the endosome to the cytoplasm.<sup>18</sup> In comparison to viral vectors, nonviral vectors provide the advantage that they can be easily synthesized and convince especially by their absent immunogenic potential and enhanced biocompatibility.

We have recently developed a novel class of branched polyplexes based on oligoethylenimine (OEI)-grafted polypropylenimine dendrimers (G2-HD-OEI),<sup>19</sup> which showed high-intrinsic tumor affinity in the presence of low toxicity and high transfection efficiency.<sup>19,20</sup> In a syngeneic neuroblastoma (Neuro2A) mouse model we have used these synthetic polymeric vectors to target NIS expression to neuroblastoma tumors. After intravenous (i.v.) application of NIS-containing polyplexes (G2-HD-OEI/NIS) Neuro2A tumors were shown to accumulate 8–13% injected dose per gram (ID/g) <sup>125</sup>I by scintigraphy and *ex-vivo* gamma counting, resulting in a tumor-absorbed dose of 247 mGray/Megabecquerel (mGy/MBq) <sup>131</sup>I. No iodide uptake was observed in nontarget organs and two cycles of polyplex application followed by <sup>131</sup>I (55.5 MBq) administration resulted in a significant delay in tumor growth associated with markedly improved survival.<sup>11</sup> Polyplexes formed with branched structures like G2-HD-OEI are able to deliver the nucleic acid payload primarily toward the tumor site due to passive tumor targeting based on the imperfect and leaky tumor vasculature combined with inadequate lymphatic drainage.<sup>21</sup>

With the aim of optimizing tumor selectivity active ligand-mediated tumor targeting by the application of receptor-specific ligands can be used. The epidermal growth factor receptor (EGFR) is upregulated in a broad range of epithelial tumors, such as liver cancer, and has therefore been evaluated as a target structure for gene delivery vectors.<sup>22</sup> Epidermal growth factor (EGF), the natural ligand of the EGFR, has strong growth promoting properties by activation of the receptor tyrosine kinase via phosphorylation and thereby represents a strong tumor-promoting agent. Therefore, a synthetic ligand with high-receptor affinity, which does not activate the receptor tyrosine kinase is required to function as a plausible ligand to target gene delivery vectors to EGFR-expressing tumor cells. In this context, Li *et al.* discovered a new EGFR ligand by phage display library analysis called GE11 (sequence: YHWYGYTPQNVI) which showed high affinity toward EGFR with no significant activation potential at the receptor tyrosine kinase.<sup>23</sup>

In the present study, we therefore used novel synthetic nanoparticle vectors based on linear polyethylenimine (LPEI), shielded by attachment of polyethylene glycol (PEG) and coupled with the synthetic EGFR-specific peptide GE11 for targeting the NIS gene to human hepatocellular carcinoma (HCC)

cells. Based on its dual function as reporter and therapy gene, NIS was used for noninvasive imaging of vector biodistribution by <sup>125</sup>I-scintigraphy followed by assessment of the therapy response after application of <sup>131</sup>I.

## RESULTS

### EGFR-targeted NIS gene transfer *in vitro*

Transfection conditions using LPEI-PEG-GE11/NIS were optimized in HuH7 cells by measurement of perchlorate-sensitive iodide uptake activity 24 hours following application of polyplexes (data not shown). We found an optimal conjugate/plasmid ratio of 0.8 resulting in highest transfection efficiency at lowest cytotoxicity. This ratio was used in all subsequent experiments. Twenty-four hours after transfection with LPEI-PEG-GE11/NIS, HuH7 cells showed a 22-fold increase in <sup>125</sup>I accumulation as compared to cells incubated with LPEI-PEG-GE11/antisense-NIS (Figure 1a). Transfection efficacy of LPEI-PEG-GE11/NIS correlated well with levels of EGFR expression as shown by transfection experiments with three additional cancer cell lines (SKOV-3, FTC-133, MCF-7) (Figure 1c) with high, intermediate, and very low EGFR expression levels, respectively, as determined by fluorescence-activated cell scanning analysis (Figure 1b). Transfection with untargeted LPEI-PEG-Cys (cysteine)/NIS polyplexes resulted in significantly lower

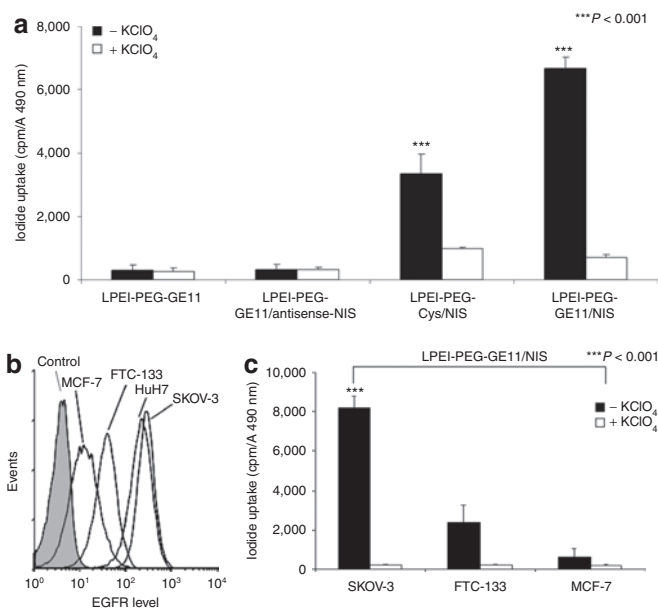


**Figure 1** Iodide uptake was measured in HuH7 cells following *in vitro* transfection with LPEI-PEG-GE11/NIS, control polyplexes LPEI-PEG-Cys/NIS, LPEI-PEG-GE11/antisense-NIS, or with LPEI-PEG-GE11 alone. Cells transfected with LPEI-PEG-GE11/NIS showed a 22-fold increase in perchlorate-sensitive <sup>125</sup>I accumulation. After transfection with LPEI-PEG-Cys/NIS the iodide uptake was decreased to ~50%. In contrast, no perchlorate-sensitive iodide uptake above background level was observed in cells transfected with LPEI-PEG-GE11/antisense-NIS or without DNA (\*\*\**P* < 0.001) (Figure 1a). Transfection efficacy of LPEI-PEG-GE11/NIS was confirmed in additional cancer cell lines and correlated with EGFR expression levels as shown in cell lines with high (SKOV-3), intermediate (FTC-133), and very low (MCF-7) EGFR expression (Figure 1b,c) which was determined by fluorescence-activated cell scanning analysis (Figure 1b). Cys, cysteine; EGFR, epidermal growth factor receptor; LPEI, linear polyethylenimine; NIS, sodium iodide symporter; PEG, polyethylene glycol.

iodide uptake activity in HuH7 cells (Figure 1a). Furthermore, no perchlorate-sensitive iodide uptake above background level was observed in cells transfected with the empty vector LPEI-PEG-GE11. Polyplex-mediated NIS gene transfer did not alter cell viability as measured by MTS assay (Figure 1a).

### Induction of iodide accumulation after systemic EGFR-targeted NIS gene transfer *in vivo*

To investigate the iodide uptake activity in HuH7 tumors after systemic *in vivo* NIS gene transfer,  $^{123}\text{I}$  distribution was monitored in tumor-bearing mice 24 hours after administration of polyplexes (Figure 2). High levels of iodide uptake were observed in 80% (12 out of 15) of HuH7 tumors following systemic injection of LPEI-PEG-GE11/NIS (Figure 2a), whereas no significant iodide uptake was observed in nontarget organs, including lungs and liver confirming tumor-specificity of LPEI-PEG-GE11-mediated NIS gene delivery. No iodide accumulation was detected in tumors after application of LPEI-PEG-GE11/antisense-NIS and LPEI/NIS (Figure 2c,e), and weak tumoral iodide accumulation was observed after application of LPEI-PEG-Cys/NIS (Figure 2d). To confirm that tumoral iodide uptake was indeed NIS-mediated, LPEI-PEG-GE11/NIS-injected mice received sodium perchlorate 30 minutes before  $^{123}\text{I}$  administration [2 mg intraperitoneally (i.p.)], which completely blocked tumoral iodide accumulation in addition to the physiological iodide uptake in stomach and thyroid gland (Figure 2b). As determined by serial scanning,  $\sim 6.5\text{--}9\%$  ID/g  $^{123}\text{I}$  was accumulated in NIS-transduced tumors with a biological half-life of 5 hours after application of LPEI-PEG-GE11/NIS (Figure 2g). Considering a tumor mass of 1 g and an effective half-life of 6 hours for  $^{131}\text{I}$ , a tumor-absorbed dose of 47 mGy/MBq  $^{131}\text{I}$  was calculated. After application of the EGFR-specific antibody cetuximab 24 hours before administration of NIS-conjugated LPEI-PEG-GE11 tumoral iodide uptake was significantly reduced to 4% ID/g  $^{123}\text{I}$  (Figure 2f).

Besides tumoral uptake, significant radioiodine accumulation was observed in tissues physiologically expressing NIS, including stomach and thyroid, as well as in the urinary bladder (average of  $\sim 10\%$  ID, depending on diuretic activity) due to elimination of radioiodine through the kidneys. In this context, it is important to mention that due to exquisite regulation of thyroidal NIS expression by thyroid-stimulating hormone,  $^{123}\text{I}$  accumulation in the thyroid gland can effectively be downregulated by thyroid hormone treatment as shown in humans.<sup>24</sup> In addition, by stimulation of diuresis the radioiodine retention time in the bladder can be effectively shortened thereby minimizing the delivered dose and avoiding side effects to the bladder and adjacent tissues. In the past 70 years of routine radioiodine application in thyroid cancer patients, no major adverse effects have therefore been observed in the urinary tract including kidney, bladder, or neighboring tissues.

### *Ex vivo* radioiodine biodistribution studies

*Ex vivo* biodistribution analysis confirmed induction of significant iodide uptake activity in tumors by systemic NIS gene transfer (Figure 3). LPEI-PEG-GE11/NIS-transduced HuH7 tumors accumulated 4.3% ID/organ  $^{123}\text{I}$  4 hours after radioiodine injection (Figure 3a), whereas tumors transduced with control polyplexes

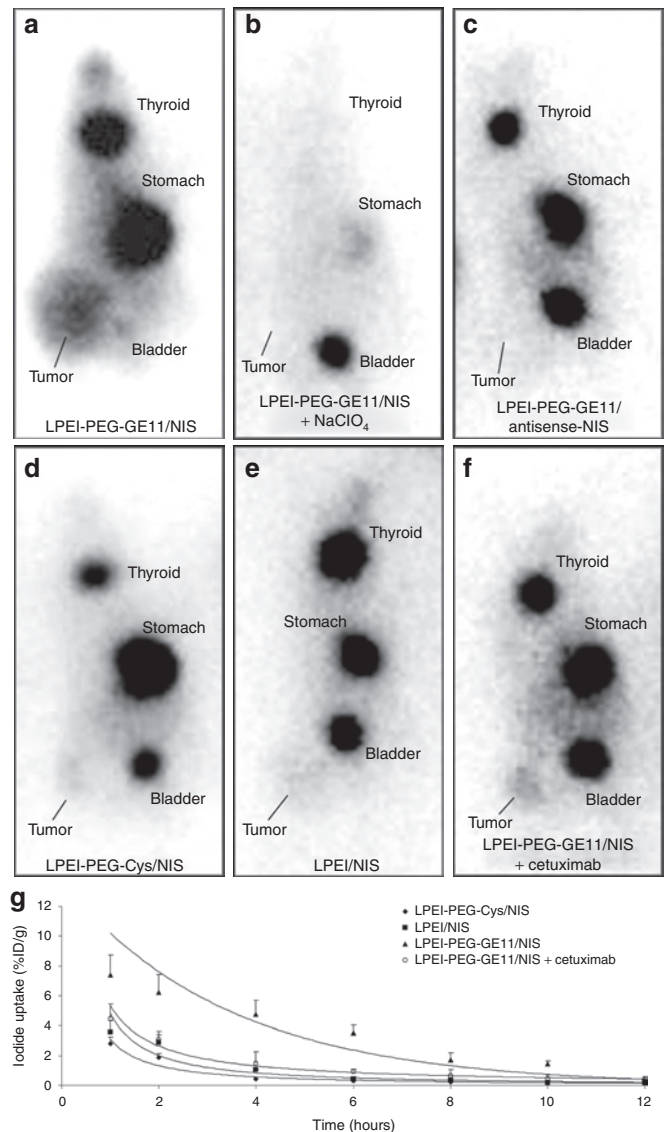


**Figure 2**  $^{123}\text{I}$  gamma camera imaging of mice harboring HuH7 tumors 3 hours following intraperitoneal (i.p.) injection of 18.5 MBq  $^{123}\text{I}$  24 hours after LPEI-PEG-GE11-mediated NIS gene delivery. While mice treated with control polyplexes (LPEI-PEG-GE11/antisense-NIS, LPEI/NIS) showed no tumoral iodide uptake (c,e), treatment with LPEI-PEG-Cys/NIS led to a mild iodide uptake of 2.4% injected dose per gram (ID/g) (d). Treatment with (a) LPEI-PEG-GE11/NIS induced significant tumoral iodide accumulation in HuH7 tumors with accumulation of 6.5–9% ID/g  $^{123}\text{I}$ , which was completely abolished upon pretreatment with (b)  $\text{NaClO}_4$ . Iodide was also accumulated physiologically in thyroid, stomach, and bladder (a,c,d,e,f). (f) After pretreatment with cetuximab, the iodide uptake was significantly reduced to 4% ID/g. Time course of  $^{123}\text{I}$  accumulation in HuH7 tumors after systemic polyplex-mediated NIS gene delivery followed by injection of 18.5 MBq  $^{123}\text{I}$  as determined by serial scanning. After application of LPEI-PEG-GE11/NIS, the maximum tumoral radioiodine uptake was 6.5–9% ID/g tumor with an average effective  $t_{1/2}$  of 6 hours for  $^{131}\text{I}$ . Following injection of control polyplexes (LPEI-PEG-Cys/NIS, LPEI/NIS) or after pretreatment with cetuximab iodide accumulation was significantly decreased (g). Cys, cysteine; LPEI, linear polyethylenimine; NIS, sodium iodide symporter; PEG, polyethylene glycol.

(LPEI-PEG-Cys/NIS, LPEI-PEG-GE11/antisense-NIS, and LPEI/NIS) showed only mild (LPEI-PEG-Cys/NIS) or no (LPEI/NIS, LPEI-PEG-GE11/antisense-NIS) iodide uptake. In all groups, the

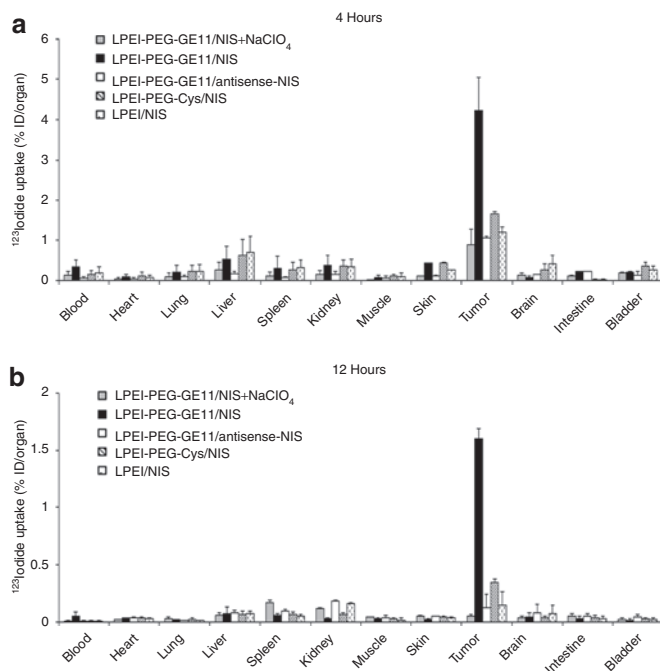


**Figure 3** Evaluation of iodide biodistribution *ex vivo* (a) 4 hours and (b) 12 hours following injection of 18.5 MBq  $^{123}\text{I}$ . While tumors in sodium iodide symporter (NIS)-transduced mice showed high perchlorate-sensitive iodide uptake activity [up to 4.3% injected dose per organ (ID/organ)], nontarget organs revealed no significant iodide accumulation. No iodide accumulation was measured after injection of control polyplexes LPEI-PEG-GE11/antisense-NIS or LPEI/NIS, or after pretreatment with  $\text{NaClO}_4$ . A mild iodide uptake was observed after application of LPEI-PEG-Cys/NIS. Results were reported as percent of injected dose per organ  $\pm$  SD. Cys, cysteine; LPEI, linear polyethylenimine; NIS, sodium iodide symporter; PEG, polyethylene glycol.

thyroid gland and the stomach accumulated  $\sim 40\%$  and  $39\%$  ID/organ (data not shown). Furthermore, a single perchlorate injection before radioiodine application significantly blocked iodide uptake in NIS-transduced tumors and in physiologically NIS-expressing tissues, including thyroid and stomach, throughout the observation period up to 12 hours (Figure 3b). No iodide uptake above background level was observed in nontarget organs, including lungs, liver, kidneys, or spleen.

### Analysis of NIS mRNA expression by quantitative real-time PCR analysis

In order to assess NIS mRNA levels after systemic NIS gene transfer, mRNA of various tissues was extracted and analyzed by quantitative real-time PCR (qPCR) with a pair of NIS-specific oligonucleotide primers 24 hours after NIS gene transfer. Significant levels of NIS gene expression were induced in HuH7 tumors after systemic injection of LPEI-PEG-GE11/NIS (Figure 4a), whereas only low background levels were detected after application of LPEI-PEG-GE11/antisense-NIS, LPEI-PEG-Cys/NIS, and LPEI/NIS. As expected, administration of the competitive NIS-inhibitor sodium perchlorate had no influence on NIS mRNA expression in NIS-transduced tumors. After application of the EGFR-specific antibody cetuximab tumoral, NIS mRNA expression was significantly reduced. Furthermore, analysis of nontarget organs like lungs and liver, showed no significant NIS mRNA expression

above background level (Figure 4a). In contrast, high levels of NIS mRNA were detected in the lungs of mice receiving LPEI/NIS suggesting unspecific pulmonary accumulation of these polyplexes due to their aggregation with erythrocytes (Figure 4a).

### Analysis of NIS protein expression in HuH7 tumors

Immunohistochemical analysis of HuH7 tumors after systemic application of LPEI-PEG-GE11/NIS revealed a heterogeneous staining pattern with clusters of primarily membrane-associated NIS-specific immunoreactivity (Figure 4b). In contrast, tumors treated with LPEI-PEG-GE11/antisense-NIS, LPEI-PEG-Cys/NIS, and LPEI/NIS (Figure 4c–e) showed no NIS-specific immunoreactivity. Specificity of staining was confirmed using isotype-matched control immunoglobulin (data not shown).

### Radioiodine therapy studies after *in vivo* NIS gene transfer

Twenty-four hours after systemic administration of polyplexes, a therapeutic dose of 55.5 MBq (1.5 mCurie)  $^{131}\text{I}$  or saline was administered. The cycle consisting of systemic NIS gene transfer followed by radioiodine was repeated twice on days 3/4 and 7/8. Mice treated with three cycles of LPEI-PEG-GE11/NIS and  $^{131}\text{I}$  showed a significant delay in tumor growth as compared to all control groups (Figure 5a), tumor growth started again 1 week after the last treatment. Therefore, in another therapy group a fourth therapy cycle was added at days 14/15, which further delayed tumor growth. In all control groups (LPEI-PEG-GE11/NIS or LPEI-PEG-GE11/antisense-NIS followed by saline, or LPEI-PEG-GE11/antisense-NIS followed by  $^{131}\text{I}$ ), mice showed an exponential tumor growth and had to be killed within 2 weeks after the onset of the experiments due to excessive tumor growth (Figure 5b). Fifty percent of mice survived 3–4 weeks after application of three cycles of polyplexes followed by  $^{131}\text{I}$  application; overall survival was further enhanced by addition of another cycle of polyplex/ $^{131}\text{I}$  application (Figure 5b). Importantly, none of these mice showed major adverse effects due to radionuclide or polyplex treatment in terms of lethargy or respiratory failure. However, a minor body weight loss of 3–5% was observed in mice after systemic administration of polyplexes.

### Immunofluorescence analysis

Three to four weeks after treatment, mice were sacrificed, and tumors were dissected and processed for immunofluorescence analysis using a Ki67-specific antibody (green) and an antibody against CD31 (red, labeling blood vessels) (Figure 6). NIS-transduced tumors (LPEI-PEG-GE11/NIS) (Figure 6b) exhibited a significantly lower intratumoral blood vessel density and proliferation index after  $^{131}\text{I}$  therapy when compared to mock-transduced tumors (LPEI-PEG-GE11/antisense-NIS) (Figure 6a).

### DISCUSSION

In the present study, we investigated the efficacy of novel synthetic nanoparticle vectors based on LPEI, shielded by attachment of PEG and coupled with the EGFR-specific ligand GE11 to achieve tumor-selective NIS-mediated radioiodine accumulation in a HCC mouse model. After confirmation of high transduction

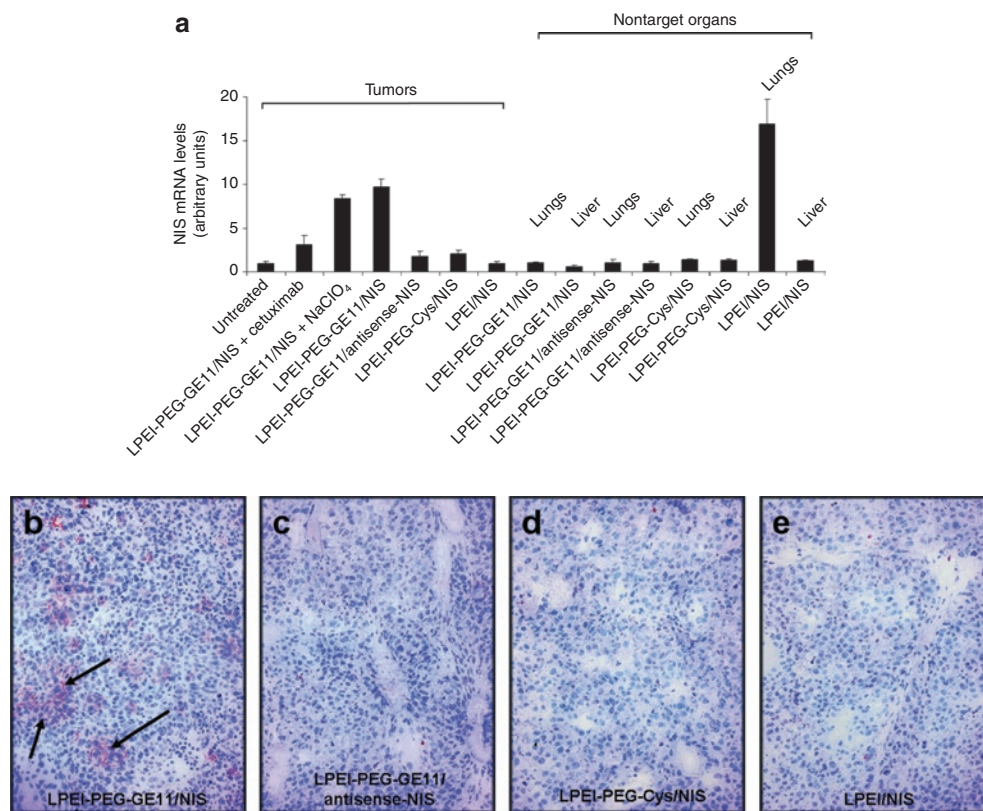


**Figure 4** Analysis of human sodium iodide symporter (NIS) mRNA expression in HuH7 tumors and nontarget organs by quantitative real-time PCR (qPCR). **(a)** A significant level of NIS mRNA expression was induced in HuH7 tumors after systemic NIS gene transfer with or without sodium perchlorate pretreatment (LPEI-PEG-GE11/NIS). Only a low background level of NIS mRNA expression was detected in untreated tumors, which was set as 1 arbitrary unit. Moreover, no significant NIS expression above background level was found in tumors after application of LPEI-PEG-GE11/antisense-NIS, LPEI-PEG-Cys/NIS, LPEI-PEG-GE11/NIS + cetuximab and LPEI/NIS. After systemic application with LPEI/NIS a high NIS mRNA expression level was detected in the lungs, whereas nontarget organs showed no significant NIS mRNA expression after treatment of LPEI-PEG-GE11/NIS, LPEI-PEG-GE11/antisense-NIS, LPEI-PEG-Cys/NIS. Results were reported as NIS/GAPDH ratios. Immunohistochemical staining of HuH7 tumors 24 hours after **(b)** LPEI-PEG-GE11/NIS application using a *hNIS*-specific antibody showed clusters of primarily membrane-associated NIS-specific immunoreactivity. In contrast, HuH7 tumors treated with the control polyplexes [**(c)** LPEI-PEG-GE11/antisense-NIS, **(d)** LPEI-PEG-Cys/NIS, **(e)** LPEI/NIS] did not reveal NIS-specific immunoreactivity. Magnification:  $\times 100$ . Cys, cysteine; LPEI, linear polyethylenimine; NIS, sodium iodide symporter; PEG, polyethylene glycol.

efficiency of LPEI-PEG-GE11 in human HCC cells *in vitro*, i.v. application of LPEI-PEG-GE11 in nude mice, carrying HCC xenografts was demonstrated to result in tumor-selective, EGFR-targeted radioiodine accumulation, which was high enough for a significant therapeutic effect after application of <sup>131</sup>I.

As one of the oldest and most successful targets of molecular imaging and therapy, cloning and characterization of NIS has provided us with a powerful new reporter and therapy gene.<sup>1,2</sup> Many of the characteristics of NIS, which have been confirmed by our work to date, suggest that it represents an ideal therapy gene due to several advantages. NIS as an endogenous human protein implies that its expression in cancer cells is unlikely to be toxic or to elicit a significant immune response that could limit its efficacy. In its dual role as reporter and therapy gene NIS allows direct, noninvasive imaging of functional NIS expression by <sup>123</sup>I-scintigraphy and <sup>124</sup>I-PET-imaging, as well as exact dosimetric calculations before proceeding to therapeutic application of <sup>131</sup>I.<sup>2</sup>

The capacity of the NIS gene to induce radioiodine accumulation in nonthyroidal tumors has been investigated by several groups including our own, demonstrating the enormous

potential of NIS as therapy gene.<sup>2-9,12,13,16,25-31</sup> However, only a limited number of studies have investigated systemic NIS gene delivery approaches to address one of the major hurdles on the way to efficient and safe application of the NIS gene therapy concept in the clinical setting in metastatic disease, which is optimal tumor targeting in the presence of low toxicity and high transduction efficiency with the ultimate goal of systemic vector application. In its function as reporter gene NIS provides an elegant means for noninvasive monitoring of vector biodistribution as well as biodistribution, level, and duration of transgene expression after systemic vector application.<sup>17,26,32,33</sup> We recently reported a systemic nonviral NIS gene delivery approach in a neuroblastoma mouse model (Neuro2A), where biodegradable branched polyplexes based on OEI-grafted polypropylenimine dendrimers (G2-HD-OEI) for systemic NIS gene application achieved tumor-specific iodide accumulation resulting in a significant therapeutic effect after application of <sup>131</sup>I even in the absence of iodide organification.<sup>11</sup> This study showed for the first time a significant therapeutic effect of radioiodine after systemic nonviral NIS gene transfer in an experimental tumor model. The high intrinsic tumor affinity

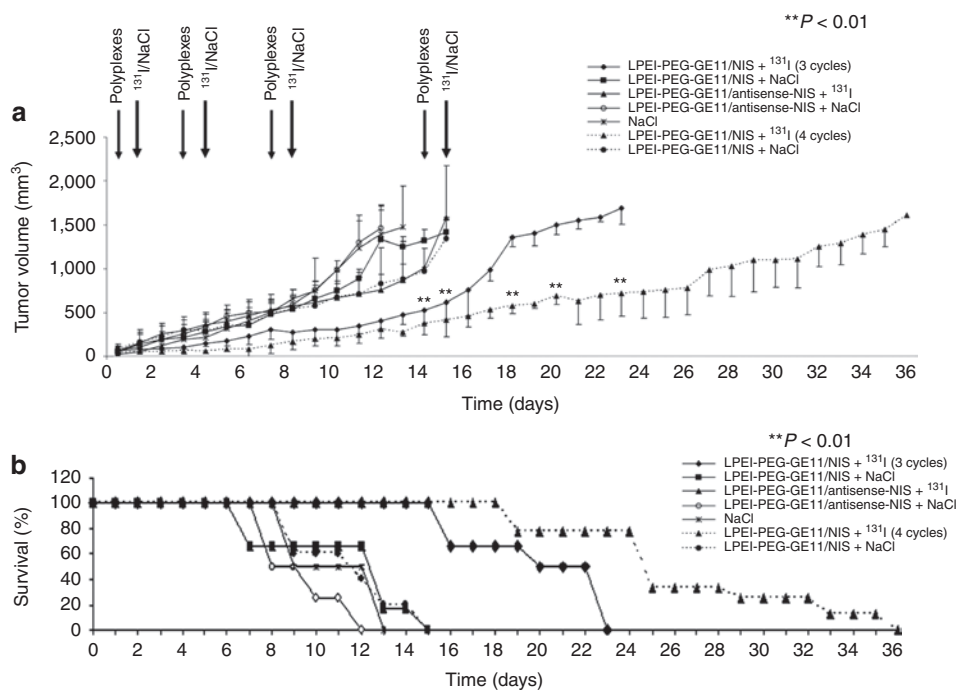


**Figure 5** Radioiodine treatment of HuH7 tumors after systemic polyplex-mediated sodium iodide symporter (NIS) gene transfer *in vivo*. Twenty-four hours after intravenous (i.v.) polyplex injection (small arrow), 55.5 MBq <sup>131</sup>I were injected intraperitoneally (i.p.) (big arrow). This treatment cycle was repeated twice on days 3/4 and 7/8 and additionally on days 14/15 (dotted lines). <sup>131</sup>I therapy after systemic LPEI-PEG-GE11/NIS application resulted in a significant delay in tumor growth (**a**,  $**P < 0.01$ ) which was associated with markedly improved survival [**b**, Kaplan–Meier plot ( $**P < 0.01$ )] as compared to the control groups that were injected with saline only, with LPEI-PEG-GE11/NIS followed by saline application, or with LPEI-PEG-GE11/antisense-NIS followed by saline or <sup>131</sup>I application. Cys, cysteine; LPEI, linear polyethylenimine; NIS, sodium iodide symporter; PEG, polyethylene glycol.

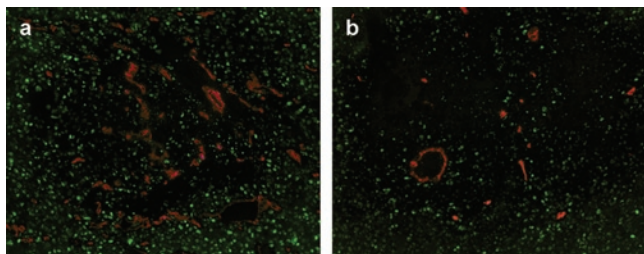


**Figure 6** Immunofluorescence analysis using a Ki67-specific antibody (green) and an antibody against CD31 (red, labeling blood vessels) showed significantly decreased proliferation and blood vessel density in (**b**) sodium iodide symporter (NIS)-transduced tumors following <sup>131</sup>I treatment as compared to (**a**) mock-transduced tumors. Slides were counterstained with DAPI nuclear stain. Magnification:  $\times 100$ .

of G2-HD-OEI is based on passive polyplex trapping in the tumor caused by the typically leaky vasculature and inadequate lymphatic drainage in tumors,<sup>21</sup> which can be highly dependent on the tumor type.<sup>34</sup>

The “golden standard” of PEI-based gene carriers is LPEI, the linear form of PEI, with a molecular weight of 22 kDa, also known as the commercially available JetPEI. The major drawback of LPEI is its significant toxicity after systemic application due to acute and long-term toxic effects.<sup>35</sup> Transgene expression was demonstrated to be  $>100$  times higher in the lung than in the tumor most probably due to pronounced aggregation with erythrocytes that usually results in high-transgene expression in the first vascular bed encountered, namely the lung.<sup>19,20</sup>

A technique to reduce unspecific toxicity and prolong blood circulation time is shielding of polyplexes by PEGylation (PEG). Zintchenko *et al.* showed in a previous study with quantoplexes (polyplexes consisting of PEI and DNA with incorporated negatively charged near-infrared-emitting cadmium telluride quantum dots), that PEGylated quantoplexes have a circulation time in the range of several minutes, whereas unshielded PEI polyplexes do not show circulation at all.<sup>36</sup> The modification of the surface of DNA complexes with PEG can block the interaction with plasma components and erythrocytes and strongly changes the *in vivo* characteristics of particles, resulting in reduced toxicity, prolonged circulation, and gene expression in distant tumor tissue after systemic administration.<sup>37</sup> However, PEGylation also results in decreased cell-binding capacity and subsequently reduced efficacy.<sup>37</sup> The addition of specific targeting ligands, such as peptides, proteins, and carbohydrates to these shielded polyplexes can be employed with the aim of active tumor targeting thereby enhancing transfection efficiency and tumor selectivity.<sup>22</sup>

In the present study, the EGFR was used as tumor-specific target, a transmembrane receptor with intrinsic tyrosine kinase activity. The upregulation to  $2 \times 10^6$  EGFR/cell in numerous solid tumors including lung, liver, breast, and bladder cancer, glioblastoma as well as HCC makes it an attractive target for cancer gene therapy strategies. EGFR-targeting has been utilized for targeted delivery of neutralizing antibodies,<sup>38</sup> toxins,<sup>39</sup> and nucleic acids,<sup>40</sup> as well as for targeted gene delivery, either with viral<sup>41</sup> or nonviral gene delivery systems.<sup>42</sup> The enhanced uptake of EGF-coupled

polyplexes in EGFR-overexpressing tumor cells was shown in several experiments with an up to 300-fold increased transfection efficiency depending on the tumor cell line.<sup>43</sup> Studies with HuH7 HCC cells showed that 50% of these “artificial viruses” were already internalized after 5 minutes, whereas untargeted polyplexes reached only ~20% after a 20-minute incubation.<sup>22</sup> Generating polyplexes with EGF as targeting ligand combined with PEG as shielding moiety lead to rapid internalization via the EGF-receptor and significantly increased transgene expression in subcutaneous hepatoma tumors in mice after systemic administration.<sup>42</sup>

EGF, the natural ligand of the EGFR, however, has strong mitogenic and neoangiogenic activity possibly attenuating the anticancer effect of the therapeutic gene used.<sup>23</sup> For this purpose, Li *et al.* screened a phage display library to discover new EGFR binders and have found a phage clone encoding for a peptide termed GE11, which showed high affinity toward EGFR without activation of the receptor tyrosine kinase. GE11-conjugated PEI polyplexes showed high transfection efficiency in EGFR-overexpressing tissues, whereas no significant activation of EGFR and no mitogenic activity of treated cells was observed.<sup>23</sup>

In our study, we used LPEI-PEG-GE11 polymers and complexed them with the human NIS complementary DNA (cDNA) under the control of the strong human elongation factor 1 $\alpha$  promoter. The plasmid used is completely devoid of CpG islands, which has been described to result in prolonged and higher transgene expression in tumor tissue *in vivo*.<sup>34,44</sup> *In vitro* transfection of HuH7 cells with LPEI-PEG-GE11/NIS resulted in a 22-fold increase in iodide uptake activity, which was significantly lower when polyplexes without EGFR-targeting (LPEI-PEG-Cys/NIS) were used. We have also confirmed high transduction efficacy of LPEI-PEG-GE11/NIS in additional cancer cell lines, including thyroid, breast, and ovarian cancer cells, demonstrating good correlation of achieved iodide accumulation with levels of EGFR expression. Following *i.v.* application of LPEI-PEG-GE11/NIS polyplexes in mice carrying HuH7 xenografts 80% of tumors showed tumor-specific <sup>123</sup>I accumulation with ~6.5–9% ID/g, a biological half-life of 6 hours, and a tumor-absorbed dose of 47 mGy/MBq <sup>131</sup>I. In addition, our *in vivo* <sup>123</sup>I scintigraphic imaging studies were confirmed by *ex vivo* biodistribution experiments revealing significant tumoral radioiodine accumulation, whereas no iodide uptake was measured in nontarget organs like liver, spleen, and lungs.

Significance of EGFR-mediated NIS gene delivery was shown in mice pretreated with the EGFR-specific antibody cetuximab 24 hours before polyplex application. Cetuximab has been shown to inhibit EGFR-mediated tumor cell targeting *in vitro* with EGF-targeted nanoparticles<sup>45</sup> and to downregulate EGFR *in vitro* and *in vivo*.<sup>46</sup> Here, we demonstrate that cetuximab pretreatment is able to reduce tumor-specific transfection efficiency of EGFR-targeted polyplexes. In line with these results, untargeted LPEI-PEG-Cys/NIS also showed significantly lower iodide uptake, further confirming the EGFR-specificity of LPEI-PEG-GE11. The low, but measurable iodide uptake activity in HCC tumors after LPEI-PEG-Cys/NIS treatment suggests that passive tumor targeting due to the “enhanced permeability and retention effect” is sufficient for a low level of tumoral NIS transduction,<sup>21</sup> which

can be significantly increased after coupling to the EGFR-specific ligand GE11. These data are consistent with the study by Song *et al.* showing enhanced extent and duration of accumulation of fluorescence-labeled liposomes-containing GE11 when compared to an unrelated peptide, where accumulation was significant, but less pronounced.<sup>47</sup> In mice treated with LPEI-PEG-GE11/NIS and the specific NIS-inhibitor sodium perchlorate before application of radioiodine or in mice treated with the control vectors (LPEI-PEG-GE11/antisense-NIS) tumors showed no significant iodide uptake demonstrating that tumoral radioiodine accumulation after systemic EGFR-targeted NIS gene transfer was mediated by functional NIS protein.

We further confirmed tumor-specific NIS expression after systemic application of LPEI-PEG-GE11/NIS by qPCR, whereas after application of LPEI/NIS high levels of NIS mRNA expression were primarily detected in the lungs of treated animals. *I.v.* applied LPEI polyplexes are known to induce high-transgene expression activity in the lungs, which is due to aggregation with erythrocytes, but also high cellular toxicity.<sup>35</sup> Despite significant mRNA levels, no NIS activity was observed in lungs, which is presumably due to LPEI-mediated cell membrane damage inhibiting proper membrane trafficking of the NIS protein, which is required for functional activity. With LPEI-PEG-GE11/NIS or LPEI-PEG-Cys/NIS polyplexes, no pulmonary NIS mRNA or NIS activity was found suggesting prevention of polyplex aggregation in the lung due to PEG shielding.

In tumor sections, NIS-specific immunoreactivity was primarily membrane-associated and occurred in clusters. The patchy staining pattern nicely correlates with experiments using G2-HD-OEI polyplexes for systemic NIS gene transfer in a syngeneic neuroblastoma mouse model<sup>11</sup> and with a study using PEI-based EGF-coupled polymers for targeting the  $\beta$ -galactosidase reporter gene to HCC cells *in vivo* resulting in a heterogeneous and patchy distribution of transgene activity.<sup>42</sup>

Most importantly, systemic EGFR-targeted NIS gene transfer resulted in tumor-specific iodide uptake activity in HCC tumor-bearing mice, which was sufficiently high for a significant therapeutic effect of <sup>131</sup>I. After three to four cycles of systemic polyplex application followed by <sup>131</sup>I injection, tumor-bearing mice showed a significant delay of tumor growth associated with a significantly prolonged survival. In addition, immunofluorescence analysis showed markedly reduced proliferation associated with decreased blood vessel density inside and surrounding the tumor after systemic polyplex-mediated NIS gene transfer followed by <sup>131</sup>I application, suggesting radiation-induced tumor stroma cell damage in addition to tumor cell death. The crossfire effect of <sup>131</sup>I with a maximum path length of up to 2.4 mm might be responsible for stromal cell damage leading to reduced angiogenesis and secretion of growth-stimulatory factors, thereby enhancing therapeutic efficacy.

Based on the study by Maxon *et al.* the target dose generally considered to be necessary for a therapeutic effect in lymph node metastases of thyroid cancer is ~80 Gy.<sup>48,49</sup> However, in clinical routine the bone marrow dose limited approach of radioiodine therapy is widely used applying activities ranging from 7 to 9 GBq, whereas routine calculation of lesion-based dosimetry is not performed.<sup>49</sup> Investigators that have performed pre- or post-therapeutic

dosimetry of thyroid cancer metastases showed strong variability of tumor-absorbed doses ranging from 0.1 to 25.8 mGy/MBq (mean 3.7 mGy/MBq) (0.5–288 Gy/lesion) using planar scintigraphy or  $^{124}\text{I}$ -PET imaging.<sup>48,49</sup> In these studies most of the lesions received a dose significantly <80 Gy, whereas tumor-absorbed doses and biological responses to radiation have not correlated well.<sup>48,49</sup> In comparison, in our study after systemic polyplex-mediated NIS gene transfer a total tumor-absorbed dose of 7.8–10.4 Gy was delivered to the tumor after three to four cycles of systemic NIS gene transfer followed by  $^{131}\text{I}$  administration, which is less than the generally assumed target dose of 80 Gy, but in the range of target doses reported for  $^{131}\text{I}$  therapy in thyroid cancer and clearly high enough for a significant therapeutic effect of  $^{131}\text{I}$  in our study.

In conclusion, our data convincingly demonstrate the high potential of novel synthetic nanoparticle vectors based on LPEI, shielded by PEG, and coupled with the synthetic peptide GE11 as an EGFR-specific ligand for targeting the NIS gene to human HCC overexpressing EGFR. Based on the role of NIS as a potent and well-characterized reporter gene allowing noninvasive imaging of functional NIS expression, this study allowed detailed characterization of *in vivo* biodistribution of EGFR-targeted functional NIS expression by gamma camera imaging, which is an essential prerequisite for exact planning and monitoring of clinical gene therapy trials with the aim of individualization of the NIS gene therapy concept in the clinical setting. Tumor-specific iodide accumulation was further demonstrated to be sufficiently high for a significant delay of tumor growth associated with increased survival in HCC xenograft bearing nude mice after three to four cycles of polyplex application followed by  $^{131}\text{I}$  therapy. This study therefore opens the exciting prospect of NIS-targeted radionuclide therapy of metastatic cancer using EGFR-targeted polyplexes for systemic NIS gene delivery.

## MATERIALS AND METHODS

**Cell culture.** The human hepatoma cell line (HuH7, JCRB 0403) was cultured in DMEM/F12 medium (Invitrogen, Karlsruhe, Germany) supplemented with 10% fetal bovine serum (vol/vol) (PAA, Colbe, Germany), 5% L-glutamine (Invitrogen), and 1% penicillin/streptomycin. The human follicular thyroid carcinoma cell line FTC-133 (kindly provided by Björn E. Wenzel, University of Lübeck, Lübeck, Germany) was grown in DMEM/F12 medium (Invitrogen) supplemented with 10% fetal bovine serum (vol/vol) (PAA), and 1% penicillin/streptomycin (vol/vol) (Invitrogen). The human breast cancer cell line MCF-7 (ATCC, HTB-22) was grown in MEM (Invitrogen) supplemented with 10% fetal bovine serum (vol/vol) (PAA), 5% L-glutamine (Invitrogen), and 1% penicillin/streptomycin. The human ovarian carcinoma cell line SKOV-3 (ATCC, HTB-77) was grown in DMEM (Invitrogen) supplemented with 10% fetal bovine serum (vol/vol) (PAA) and 1% penicillin/streptomycin (vol/vol) (Invitrogen). Cells were maintained at 37°C and 5% CO<sub>2</sub> in an incubator with 95% humidity. Cell culture medium was replaced every second day and cells were passaged at 85% confluency.

**Plasmid and polymer synthesis.** The NIS cDNA has been synthesized by GENEART (Regensburg, Germany) codon-optimized for gene expression in human tissue and cloned into the plasmid pCpG-hCMV-Luc with a backbone completely devoid of potentially immune stimulatory CpG dinucleotides.<sup>34</sup> NIS transcription is driven by the human elongation factor 1 $\alpha$  promoter in combination with the human cytomegalovirus enhancer element. The LucSh transgene was replaced by NIS cDNA using restriction enzymes *NheI* and *BglIII* (NIS plasmid). NIS cDNA, digested with *NheI* and *BglIII*, was cloned into the *NheI* and *BglIII* restriction sites of pMOD-ZGFP

(Invivogen, San Diego, CA). The resulting pMOD-NIS was digested with *AvrII* and *BamHI* and religated into the *NheI* and *BglIII* restriction sites of pCpG-hCMV-Luc generating a control vector featuring NIS in antisense direction (antisense-NIS plasmid).

LPEI and LPEI-based conjugates were synthesized in analogous fashion as recently described<sup>50</sup> and will be described in detail elsewhere (A. Schäfer, A. Phanke, D. Schaffert, W. M. von Weerden, W. Rödl, A. Vetter *et al.*, manuscript in preparation). In brief, LPEI-PEG-GE11 and LPEI-PEG-Cys were synthesized by coupling heterobifunctional (poly) ethylene glycol (NHS-PEG-OPSS, 2 kDa; Rapp Polymere, Tübingen, Germany) via *N*-hydroxy succinimidyl ester onto amine groups in LPEI and were subsequently purified by cation exchange chromatography. GE11 peptide (CYHWYGYTPQNVI, >95% purity, synthesized by solid phase peptide (Biosynthan, Berlin, Germany) was coupled to the terminal OPSS group (orthopyridyl disulfide) and purified again by size exclusion chromatography (Superdex 75; GE Healthcare Europe, Freiburg, Germany). LPEI-PEG-Cys was similarly synthesized only using Cys instead of GE11 peptide. The resulting conjugates were dialyzed against HEPES-buffered saline (20 mmol/l HEPES pH 7.4, 150 mmol/l NaCl) and stored frozen at –80°C as 1–5 mg/ml stock solutions until further use.

**Polyplex formation.** Plasmid DNA was condensed with polymers at indicated conjugate/plasmid—ratios (wt/wt) in HEPES-buffered glucose [HBG: 20 mmol/l HEPES, 5% glucose (wt/vol), pH 7.4] as described previously<sup>19</sup> and incubated at room temperature for 20 minutes before use. Final DNA concentration of polyplexes for *in vitro* studies was 2  $\mu\text{g/ml}$ , for *in vivo* studies 200  $\mu\text{g/ml}$ .

**Fluorescence-activated cell scanning analysis.** For flow cytometry analysis, HuH7, SKOV-3, FTC-133, and MCF-7 cells were harvested using Trypsin/EDTA, resuspended in phosphate-buffered saline supplemented with 10% fetal calf serum and diluted to a density of  $6 \times 10^5$  cells/100  $\mu\text{l}$ . Cells were incubated with a mouse monoclonal antihuman EGFR antibody (Dako, Hamburg, Germany) or control antibody (mouse IgG; Dako) for 1.5 hours at 4°C. Cells were washed with phosphate-buffered saline + 10% fetal calf serum and incubated with Alexa-488 conjugated polyclonal goat anti-mouse antibody (Dianova, Hamburg, Germany) (1:400) for 1 hour at 4°C. To discriminate live and dead cells, propidium iodide (Sigma Aldrich, Taufkirchen, Germany) was added before acquisition. Analysis was performed on a BD fluorescence-activated cell scanning Canto II flow cytometer (BD Biosciences). Cell aggregates and small debris were excluded from analysis by appropriate gating.

**Transient transfection.** For *in vitro* transfection experiments, HuH7 cells were grown to 60–80% confluency. Cells were incubated for 4 hours with polyplexes in the absence of serum and antibiotics followed by incubation with growth medium for 24 hours. Transfection efficiency was evaluated by measurement of iodide uptake activity as described below.

**$^{125}\text{I}$  iodide uptake assay.** Following transfections, iodide uptake of HuH7 cells was determined at steady-state conditions as described previously.<sup>9</sup> Results were normalized to cell survival measured by cell viability assay (see below) and expressed as cpm/A490 nm.

**Cell viability assay.** Cell viability was measured using the commercially available MTS-assay (Promega, Mannheim, Germany) according to the manufacturer's recommendations as described previously.<sup>3</sup>

**Establishment of HuH7 xenografts.** HuH7 xenografts were established in female CD-1 nu/nu mice (Charles River, Sulzfeld, Germany) by subcutaneous injection of  $5 \times 10^6$  HuH7 cells suspended in 100  $\mu\text{l}$  phosphate-buffered saline into the flank region. Animals were maintained under specific pathogen-free conditions with access to mouse chow and water *ad libitum*. The experimental protocol was approved by the regional governmental commission for animals (Regierung von Oberbayern).



**NIS gene transfer and radioiodine studies in vivo.** Experiments started when tumors had reached a tumor size of 8–10 mm after a 10-day pretreatment with L-T4 (L-thyroxin) (i.p. injection of 2 µg L-T4/day (Henning, Sanofi-Aventis, Germany) diluted in 100 µl phosphate-buffered saline) to suppress thyroidal iodine uptake. For systemic *in vivo* NIS gene transfer polyplexes (conjugate/plasmid 0.8) were applied i.v. via the tail vein at a DNA dose of 2.5 mg/kg (50 µg DNA in 250 µl HBG); either NIS containing polyplexes (LPEI-PEG-GE11/NIS) or control polyplexes (LPEI-PEG-GE11/antisense-NIS, LPEI-PEG-Cys/NIS, and LPEI/NIS). Four groups of mice were established and treated i.v. as follows: (i) LPEI-PEG-GE11/NIS ( $n = 15$ ), (ii) LPEI-PEG-GE11/antisense-NIS ( $n = 9$ ), (iii) LPEI-PEG-Cys/NIS ( $n = 9$ ), and (iv) LPEI/NIS ( $n = 9$ ). As an additional control, mice treated with LPEI-PEG-GE11/NIS received ( $n = 9$ ) the competitive NIS-inhibitor sodium perchlorate ( $\text{NaClO}_4$  2 mg/per mouse) 30 minutes before  $^{123}\text{I}$  administration as a single i.p. application. For competitive inhibition studies the EGFR-specific monoclonal antibody cetuximab (Erbix; Merck, Darmstadt, Germany) was injected i.p. (0.25 mg/per mouse) 24 hours before the LPEI-PEG-GE11/NIS application ( $n = 4$ ). Twenty-four hours after polyplex application, mice were injected i.p. with 18.5 MBq (0.5 mCurie)  $^{123}\text{I}$  and iodide biodistribution was assessed using a gamma camera equipped with UXHR collimator (Ecam; Siemens, Erlangen, Germany) as described previously.<sup>3</sup> Regions of interest were quantified and expressed as a fraction of the total amount of applied radioiodine per gram tumor tissue. The retention time within the tumor was determined by serial scanning after radionuclide injection and dosimetric calculations were performed according to the concept of Medical Internal Radiation Dose with the dose factor of RADAR-group ([www.doseinfo-radar.com](http://www.doseinfo-radar.com)).

**Analysis of radioiodine biodistribution ex vivo.** For *ex vivo* analysis of  $^{123}\text{I}$  biodistribution, mice were injected with LPEI-PEG-GE11/NIS ( $n = 10$ ) or LPEI-PEG-GE11/antisense-NIS ( $n = 6$ ), LPEI-PEG-Cys/NIS ( $n = 6$ ), or LPEI/NIS ( $n = 6$ ) as described above followed by i.p. injection of 18.5 MBq  $^{123}\text{I}$  24 hours later. In addition, LPEI-PEG-GE11/NIS-transduced mice ( $n = 6$ ) were treated with sodium perchlorate before  $^{123}\text{I}$  administration as an additional control. Four and twelve hours after  $^{123}\text{I}$  injection, mice were sacrificed and indicated organs were dissected, weighed, and radioiodide uptake was measured in a gamma counter (five NIS-transduced animals per time point (LPEI-PEG-GE11/NIS) and three mice of each control). Results were reported as percentage of ID/organ.

**Analysis of NIS mRNA expression using qPCR.** Total RNA was isolated from HuH7 tumors or other tissues using the RNeasy Mini Kit (Qiagen, Hilden, Germany) according to the manufacturer's recommendations. Single-stranded oligo (dT)-primer cDNA was generated using Superscript III Reverse Transcriptase (Invitrogen). Following primers were used: hNIS: (5'-ACACCTTCTGGACCTTCGTG-3') and (5'-GTCGCAGTCGGTGTAGAACA-3'), GAPDH: (5'-GAGAAGGCTGGGGCTCATTT-3') and (5'-CAGTGGGGACACGGAAGG-3'). qPCR was performed with the cDNA from 1 µg RNA using the SYBR green PCR master mix (Qiagen, Hilden, Germany) in a Rotor Gene 6000 (Corbett Research; Morthlake, New South Wales, Australia). Relative expression levels were calculated using the comparative  $\Delta\Delta C_t$  method and internal GAPDH for normalization.

**Immunohistochemical analysis of NIS protein expression.** Immunohistochemical staining of frozen tissue sections derived from HuH7 tumors after systemic gene delivery was performed using a mouse monoclonal antibody directed against amino acid residues 468–643 of human NIS (kindly provided by John C. Morris, Mayo Clinic, Rochester, MN) as described previously.<sup>8</sup>

**Radioiodine therapy study in vivo.** Following a 10-day L-T4 pretreatment, mice received 55.5 MBq  $^{131}\text{I}$  as a single i.p. injection 24 hours after systemic application of LPEI-PEG-GE11/NIS ( $n = 16$ ) or LPEI-

PEG-GE11/antisense-NIS ( $n = 6$ ). As a control, mice were treated with saline instead of  $^{131}\text{I}$  after injection of LPEI-PEG-GE11/NIS ( $n = 16$ ) or LPEI-PEG-GE11/antisense-NIS ( $n = 6$ ) or saline instead of polyplexes ( $n = 6$ ). Polyplex application was followed after 24 hours by  $^{131}\text{I}$  or saline application in three cycles (days 0/1, 3/4, 7/8). In additional experiments mice were treated with four cycles of LPEI-PEG-GE11 followed by radioiodine ( $n = 8$ ) or saline ( $n = 8$ ) application on days 0/1, 3/4, 7/8, and 14/15. Tumor sizes were measured before treatment and daily thereafter for up to 5 weeks and tumor volume estimated using the equation: tumor volume = length  $\times$  width  $\times$  height  $\times$  0.52.

**Indirect immunofluorescence assay.** Indirect immunofluorescence staining was performed on frozen tissues using an antibody against human Ki67 (Abcam, Cambridge, UK) and an antibody against mouse CD31 (BD Pharmingen, Heidelberg, Germany) as described previously.<sup>3</sup>

**Statistical methods.** All *in vitro* experiments were carried out in triplicates. Results are represented as mean  $\pm$  SD of triplicates. Statistical significance was tested using Student's *t*-test.

## ACKNOWLEDGMENTS

The authors are grateful to S. M. Jhiang, Ohio State University, Columbus, OH, for supplying the full-length human NIS cDNA and to J.C. Morris, Mayo Clinic, Rochester, MN, for providing the NIS mouse monoclonal antibody. We also thank W. Münzing (Department of Nuclear Medicine, Ludwig-Maximilians-University, Munich, Germany) for assistance with imaging studies. Wolfgang Rödl is gratefully acknowledged for conjugate synthesis and Arzu Cengizeroglu for help with plasmid production. We are grateful to Alexandra Vetter for help with FACS analysis. This study was supported by grant SFB 824 (Sonderforschungsbereich 824) from the Deutsche Forschungsgemeinschaft, Bonn, Germany to C.S. and M.O., and by a grant from the Wilhelm-Sander-Stiftung (2008.037.1) to C.S.

## REFERENCES

- Hingorani, M, Spitzweg, C, Vassaux, G, Newbold, K, Melcher, A, Pandha, H *et al.* (2010). The biology of the sodium iodide symporter and its potential for targeted gene delivery. *Curr Cancer Drug Targets* **10**: 242–267.
- Spitzweg, C and Morris, JC (2002). The sodium iodide symporter: its pathophysiological and therapeutic implications. *Clin Endocrinol (Oxf)* **57**: 559–574.
- Willhauck, MJ, Sharif Samani, BR, Gildehaus, FJ, Wolf, I, Senekowitsch-Schmidtke, R, Stark, HJ *et al.* (2007). Application of  $^{188}\text{Re}$  as an alternative radionuclide for treatment of prostate cancer after tumor-specific sodium iodide symporter gene expression. *J Clin Endocrinol Metab* **92**: 4451–4458.
- Willhauck, MJ, Samani, BR, Wolf, I, Senekowitsch-Schmidtke, R, Stark, HJ, Meyer, GJ *et al.* (2008). The potential of  $^{211}\text{At}$  for NIS-mediated radionuclide therapy in prostate cancer. *Eur J Nucl Med Mol Imaging* **35**: 1272–1281.
- Spitzweg, C, Dietz, AB, O'Connor, MK, Bergert, ER, Tindall, DJ, Young, CY *et al.* (2001). *In vivo* sodium iodide symporter gene therapy of prostate cancer. *Gene Ther* **8**: 1524–1531.
- Spitzweg, C, O'Connor, MK, Bergert, ER, Tindall, DJ, Young, CY and Morris, JC (2000). Treatment of prostate cancer by radioiodine therapy after tissue-specific expression of the sodium iodide symporter. *Cancer Res* **60**: 6526–6530.
- Willhauck, MJ, Sharif Samani, BR, Klutz, K, Cengic, N, Wolf, I, Mohr, L *et al.* (2008).  $\alpha$ -Fetoprotein promoter-targeted sodium iodide symporter gene therapy of hepatocellular carcinoma. *Gene Ther* **15**: 214–223.
- Spitzweg, C, Baker, CH, Bergert, ER, O'Connor, MK and Morris, JC (2007). Image-guided radioiodide therapy of medullary thyroid cancer after carcinoembryonic antigen promoter-targeted sodium iodide symporter gene expression. *Hum Gene Ther* **18**: 916–924.
- Spitzweg, C, Zhang, S, Bergert, ER, Castro, MR, McIver, B, Heufelder, AE *et al.* (1999). Prostate-specific antigen (PSA) promoter-driven androgen-inducible expression of sodium iodide symporter in prostate cancer cell lines. *Cancer Res* **59**: 2136–2141.
- Baril, P, Martin-Duque, P and Vassaux, G (2010). Visualization of gene expression in the live subject using the Na/I symporter as a reporter gene: applications in biotherapy. *Br J Pharmacol* **159**: 761–771.
- Klutz, K, Russ, V, Willhauck, MJ, Wunderlich, N, Zach, C, Gildehaus, FJ *et al.* (2009). Targeted radioiodine therapy of neuroblastoma tumors following systemic nonviral delivery of the sodium iodide symporter gene. *Clin Cancer Res* **15**: 6079–6086.
- Trujillo, MA, Oneal, MJ, McDonough, S, Qin, R and Morris, JC (2010). A probasin promoter, conditionally replicating adenovirus that expresses the sodium iodide symporter (NIS) for radiovirotherapy of prostate cancer. *Gene Ther* **17**: 1325–1332.
- Peerlinck, I, Merron, A, Baril, P, Conchon, S, Martin-Duque, P, Hindorf, C *et al.* (2009). Targeted radionuclide therapy using a Wnt-targeted replicating adenovirus encoding the Na/I symporter. *Clin Cancer Res* **15**: 6595–6601.

14. Groot-Wassink, T, Aboagye, EO, Wang, Y, Lemoine, NR, Reader, AJ and Vassaux, G (2004). Quantitative imaging of Na/I symporter transgene expression using positron emission tomography in the living animal. *Mol Ther* **9**: 436–442.
15. Watanabe, Y, Horie, S, Funaki, Y, Kikuchi, Y, Yamazaki, H, Ishii, K *et al.* (2010). Delivery of Na/I symporter gene into skeletal muscle using nanobubbles and ultrasound: visualization of gene expression by PET. *J Nucl Med* **51**: 951–958.
16. Li, H, Peng, KW, Dingli, D, Kratzke, RA and Russell, SJ (2010). Oncolytic measles viruses encoding interferon beta and the thyroidal sodium iodide symporter gene for mesothelioma virotherapy. *Cancer Gene Ther* **17**: 550–558.
17. Goel, A, Carlson, SK, Classic, KL, Greiner, S, Naik, S, Power, AT *et al.* (2007). Radioiodide imaging and radiovirotherapy of multiple myeloma using VSV(Delta51)-NIS, an attenuated vesicular stomatitis virus encoding the sodium iodide symporter gene. *Blood* **110**: 2342–2350.
18. Meyer, M and Wagner, E (2006). Recent developments in the application of plasmid DNA-based vectors and small interfering RNA therapeutics for cancer. *Hum Gene Ther* **17**: 1062–1076.
19. Russ, V, Günther, M, Halama, A, Ogris, M and Wagner, E (2008). Oligoethylenimine-grafted polypropylenimine dendrimers as degradable and biocompatible synthetic vectors for gene delivery. *J Control Release* **132**: 131–140.
20. Russ, V, Elfberg, H, Thoma, C, Kloeckner, J, Ogris, M and Wagner, E (2008). Novel degradable oligoethylenimine acrylate ester-based pseudodendrimers for *in vitro* and *in vivo* gene transfer. *Gene Ther* **15**: 18–29.
21. Maeda, H (2001). The enhanced permeability and retention (EPR) effect in tumor vasculature: the key role of tumor-selective macromolecular drug targeting. *Adv Enzyme Regul* **41**: 189–207.
22. de Bruin, K, Ruthardt, N, von Gersdorff, K, Bausinger, R, Wagner, E, Ogris, M *et al.* (2007). Cellular dynamics of EGF receptor-targeted synthetic viruses. *Mol Ther* **15**: 1297–1305.
23. Li, Z, Zhao, R, Wu, X, Sun, Y, Yao, M, Li, J *et al.* (2005). Identification and characterization of a novel peptide ligand of epidermal growth factor receptor for targeted delivery of therapeutics. *FASEB J* **19**: 1978–1985.
24. Wapnir, IL, Goris, M, Yudd, A, Dohan, O, Adelman, D, Nowels, K *et al.* (2004). The Na<sup>+</sup>/I<sup>-</sup> symporter mediates iodide uptake in breast cancer metastases and can be selectively down-regulated in the thyroid. *Clin Cancer Res* **10**: 4294–4302.
25. Kakinuma, H, Bergert, ER, Spitzweg, C, Chevill, JC, Lieber, MM and Morris, JC (2003). Probasin promoter (ARR(2)PB)-driven, prostate-specific expression of the human sodium iodide symporter (h-NIS) for targeted radioiodine therapy of prostate cancer. *Cancer Res* **63**: 7840–7844.
26. Dingli, D, Peng, KW, Harvey, ME, Greipp, PR, O'Connor, MK, Cattaneo, R *et al.* (2004). Image-guided radiovirotherapy for multiple myeloma using a recombinant measles virus expressing the thyroidal sodium iodide symporter. *Blood* **103**: 1641–1646.
27. Dwyer, RM, Bergert, ER, O'Connor, MK, Gendler, SJ and Morris, JC (2006). Adenovirus-mediated and targeted expression of the sodium-iodide symporter permits *in vivo* radioiodide imaging and therapy of pancreatic tumors. *Hum Gene Ther* **17**: 661–668.
28. Hingorani, M, White, CL, Zaidi, S, Pandha, HS, Melcher, AA, Bhide, SA *et al.* (2010). Therapeutic effect of sodium iodide symporter gene therapy combined with external beam radiotherapy and targeted drugs that inhibit DNA repair. *Mol Ther* **18**: 1599–1605.
29. Dwyer, RM, Bergert, ER, O'Connor, MK, Gendler, SJ and Morris, JC (2005). *In vivo* radioiodide imaging and treatment of breast cancer xenografts after MUC1-driven expression of the sodium iodide symporter. *Clin Cancer Res* **11**: 1483–1489.
30. Scholz, IV, Cengic, N, Baker, CH, Harrington, KJ, Maletz, K, Bergert, ER *et al.* (2005). Radioiodine therapy of colon cancer following tissue-specific sodium iodide symporter gene transfer. *Gene Ther* **12**: 272–280.
31. Cengic, N, Baker, CH, Schütz, M, Göke, B, Morris, JC and Spitzweg, C (2005). A novel therapeutic strategy for medullary thyroid cancer based on radioiodine therapy following tissue-specific sodium iodide symporter gene expression. *J Clin Endocrinol Metab* **90**: 4457–4464.
32. Liu, C, Russell, SJ and Peng, KW (2010). Systemic therapy of disseminated myeloma in passively immunized mice using measles virus-infected cell carriers. *Mol Ther* **18**: 1155–1164.
33. Chisholm, EJ, Vassaux, G, Martin-Duque, P, Chevre, R, Lambert, O, Pitard, B *et al.* (2009). Cancer-specific transgene expression mediated by systemic injection of nanoparticles. *Cancer Res* **69**: 2655–2662.
34. Navarro, G, Maiwald, G, Haase, R, Rogach, AL, Wagner, E, de Ilarduya, CT *et al.* (2010). Low generation PAMAM dendrimer and CpG free plasmids allow targeted and extended transgene expression in tumors after systemic delivery. *J Control Release* **146**: 99–105.
35. Chollet, P, Favrot, MC, Hurlin, A and Coll, JL (2002). Side-effects of a systemic injection of linear polyethylenimine-DNA complexes. *J Gene Med* **4**: 84–91.
36. Zintchenko, A, Susa, AS, Concia, M, Feldmann, J, Wagner, E, Rogach, AL *et al.* (2009). Drug nanocarriers labeled with near-infrared-emitting quantum dots (quantoplexes): imaging fast dynamics of distribution in living animals. *Mol Ther* **17**: 1849–1856.
37. Ogris, M, Brunner, S, Schüller, S, Kircheis, R and Wagner, E (1999). PEGylated DNA/transferrin-PEI complexes: reduced interaction with blood components, extended circulation in blood and potential for systemic gene delivery. *Gene Ther* **6**: 595–605.
38. Mendelsohn, J and Baselga, J (2006). Epidermal growth factor receptor targeting in cancer. *Semin Oncol* **33**: 369–385.
39. Liu, TF, Hall, PD, Cohen, KA, Willingham, MC, Cai, J, Thorburn, A *et al.* (2005). Interstitial diphtheria toxin-epidermal growth factor fusion protein therapy produces regressions of subcutaneous human glioblastoma multiforme tumors in athymic nude mice. *Clin Cancer Res* **11**: 329–334.
40. Shir, A, Ogris, M, Wagner, E and Levitzki, A (2006). EGF receptor-targeted synthetic double-stranded RNA eliminates glioblastoma, breast cancer, and adenocarcinoma tumors in mice. *PLoS Med* **3**: e6.
41. Dmitriev, I, Kashentseva, E, Rogers, BE, Krasnykh, V and Curiel, DT (2000). Ectodomain of coxsackievirus and adenovirus receptor genetically fused to epidermal growth factor mediates adenovirus targeting to epidermal growth factor receptor-positive cells. *J Virol* **74**: 6875–6884.
42. Wolschek, MF, Thallinger, C, Kurs, M, Rössler, V, Allen, M, Lichtenberger, C *et al.* (2002). Specific systemic nonviral gene delivery to human hepatocellular carcinoma xenografts in SCID mice. *Hepatology* **36**: 1106–1114.
43. Blessing, T, Kurs, M, Holzhauser, R, Kircheis, R and Wagner, E (2001). Different strategies for formation of pegylated EGF-conjugated PEI/DNA complexes for targeted gene delivery. *Bioconjug Chem* **12**: 529–537.
44. de Wolf, HK, Johansson, N, Thong, AT, Snel, CJ, Mastrobattista, E, Hennink, WE *et al.* (2008). Plasmid CpG depletion improves degree and duration of tumor gene expression after intravenous administration of polyplexes. *Pharm Res* **25**: 1654–1662.
45. Diagaradjane, P, Orenstein-Cardona, JM, Colón-Casasnovas, NE, Deorukhkar, A, Shentu, S, Kuno, N *et al.* (2008). Imaging epidermal growth factor receptor expression *in vivo*: pharmacokinetic and biodistribution characterization of a bioconjugated quantum dot nanoprobe. *Clin Cancer Res* **14**: 731–741.
46. Perez-Torres, M, Guix, M, Gonzalez, A and Arteaga, CL (2006). Epidermal growth factor receptor (EGFR) antibody down-regulates mutant receptors and inhibits tumors expressing EGFR mutations. *J Biol Chem* **281**: 40183–40192.
47. Song, S, Liu, D, Peng, J, Sun, Y, Li, Z, Gu, JR *et al.* (2008). Peptide ligand-mediated liposome distribution and targeting to EGFR expressing tumor *in vivo*. *Int J Pharm* **363**: 155–161.
48. Chiesa, C, Castellani, MR, Vellani, C, Orunesu, E, Negri, A, Azzeroni, R *et al.* (2009). Individualized dosimetry in the management of metastatic differentiated thyroid cancer. *Q J Nucl Med Mol Imaging* **53**: 546–561.
49. Lassmann, M, Reiners, C, Luster, M, Chiesa, C, Castellani, MR, Vellani, C *et al.* (2009). Dosimetry and thyroid cancer: the individual dosage of radioiodine. *Endocr Relat Cancer* **17**: R161–R172.
50. Schaffert, D, Kiss, M, Rodl, W, Shir, A, Levitzki, A, Ogris, M *et al.* (2010). Poly(1:1)-Mediated tumor growth suppression in EGF-receptor overexpressing tumors using EGF-polyethylene glycol-linear polyethylenimine as carrier. *Pharm Res* (epub ahead of print).